Overcoming RFI with High Mask Angle Antennas and Multiple GNSS Constellations

Liang Heng[1], Todd Walter[2], Per Enge[2], and Grace Xingxin Gao[1]

1. University of Illinois at Urbana-Champaign

2. Stanford University

BIOGRAPHY

Liang Heng is a postdoctoral research associate in the Department of Aerospace Engineering, University of Illinois at Urbana-Champaign. He received the B.S. and M.S. degrees from Tsinghua University, China in 2006 and 2008, and the Ph.D. degree from Stanford University in 2012, all in Electrical Engineering. His research interests are in cooperative navigation and satellite navigation. He is a member of the Institute of Electrical and Electronics Engineer (IEEE) and the Institute of Navigation (ION).

Todd Walter is a Senior Research Engineer in the Department of Aeronautics and Astronautics at Stanford University. He received his Ph.D. in 1993 from Stanford University. His current activities include defining future architectures to provide aircraft guidance and working with the FAA on the implementation of dual-frequency WAAS. Key early contributions include: prototype development proving the feasibility of WAAS, significant contribution to WAAS MOPS, and design of integrity algorithms for WAAS. He is a fellow of the ION and served as its president.

Per Enge is a Professor of Aeronautics and Astronautics at Stanford University, where he is the Kleiner-Perkins Professor in the School of Engineering. He directs the GPS Research Laboratory, which develops satellite navigation systems based on the Global Positioning System (GPS). He has been involved in the development of WAAS and LAAS for the FAA. He has received the Kepler, Thurlow and Burka Awards from the ION for his work. He is also a member of the National Academy of Engineering and a Fellow of the IEEE and the ION. He received his PhD from the University of Illinois in 1983.

Grace Xingxin Gao is an assistant professor in the Aerospace Engineering Department at University of Illinois at Urbana-Champaign. She received her B.S. degree in Mechanical Engineering in 2001 and her M.S. degree in Electrical Engineering in 2003, both at Tsinghua University, China. She obtained her Ph.D. degree in Electrical Engineering at Stanford University in 2008. Before joining Illinois at Urbana-Champaign as an assistant professor in 2012, Prof. Gao was a research associate at Stanford University. Prof. Gao has won a number of awards, including RTCA William E. Jackson Award, Institute of Navigation Early Achievement Award, 50 GNSS Leaders to Watch by GPS World Magazine, and multiple best presentation awards at ION GNSS conferences.

ABSTRACT

Radio frequency interference (RFI) has been being a significant issue for global navigation satellite system (GNSS) users. An increasing number of satellites in multiple constellations enable users to use high mask angle antennas (HMAAs) to reduce RFI from terrestrial sources. This paper studies the optimal antenna mask angle that maximizes the suppression of RFI but still maintains the performance of a single constellation with a low mask angle antenna.

The paper first introduces a novel lower bound on expectation of DOP. Our theoretical analysis based on the lower bound generates a closed-form expression that directly relates DOP to the antenna mask angle and the average number of visible satellites. Then, we conduct numerical simulations based on actual and planned GNSS orbits. The optimal mask angles obtained from theoretical analysis highly agree with the simulation results based on similar assumptions.

The theoretical and simulation results show that two constellations can match performance of one with 5–14° higher mask, and three constellations can match performance of one with 11–23° higher mask, depending on the DOP metric and the range error model used. The results also show diminishing marginal gain of mask angle obtained with the increase in number of satellites. In addition, using HMAAs is more beneficial to users interested in positioning accuracy than users interested in time transfer accuracy.

INTRODUCTION

The Global Positioning System (GPS) signals received on the Earth are extremely weak because of the relatively low transmit power (nominally 27 W) and huge path loss (typically −158 dB) [1]. Thanks to the processing gain (typically 30 dB) obtained from despreading the pseudorandom noise codes, GPS receivers can extract the signal buried in the background noise and precisely measure pseudoranges. Herein, however, lies a problem that radio frequency (RF) signals overlapping GPS frequencies from nearby transmitters can easily raise the noise level so that the processing gain is insufficient to extract the signal. Although deliberate jamming [2] of GPS signals is prohibited in most countries, various incidents of intentional or unintentional RF interference (RFI) have occurred and continue to occur [3–7]. RFI poses a significant threat to the availability and continuity of GPS-based navigation systems. As the global information infrastructure and world's economy comes to rely more and more on GPS [8], it is of great interest to harden GPS-based navigation systems against RFI.

A variety of methods have been proposed to help GPS receivers overcome RFI. For RFI signals known to be sparse in the time and frequency domains, pre-correlation excisers can suppress interference signals through time-frequency filtering [7, 9, 10]. Unfortunately, these excisers are not very effective when RFI signals are not sparse. Antenna arrays represent a promising approach to suppressing RFI signals regardless of their sparsity. An antenna array can form beams to satellites and steer nulls to RFI transmitters, greatly improving the signal to interference plus noise ratio [11–13]. In practice, antenna arrays suffer from issues such as the bulky size, complex structure, computationally intensive receiver processing, and time-varying biases introduced by spatial and temporal filtering [14]. These drawbacks limit the use of antenna arrays, especially for airborne and handheld applications.

The development of other global navigation satellite systems (GNSS), i.e., the Russian Global'naya Navigatsionnaya Sputnikovaya Sistema (GLONASS), the European Galileo, and the Chinese Compass, enables users to use high mask angle[1] antennas (HMAAs) to overcome RFI. This method is based on the fact that RFI sources are mostly on the ground. As shown in Figure 1, a receiver equipped with a HMAA can suppress RFI and GNSS signals coming from low elevation angles. With an increased number of satellites from multiple constellations, the receiver can still comply

[1] Antenna mask angle, a parameter in GNSS antenna design, defines the elevation below which RF signals will be considerably attenuated. This should not be confused with the parameter "mask angle" or "cutoff angle" in receiver configuration for excluding low-elevation satellites from position solution.

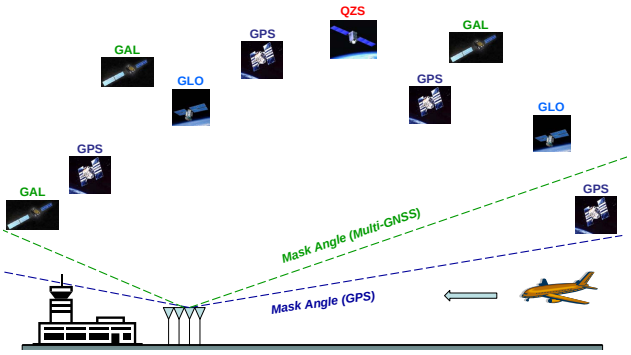

Figure 1. A simple method to overcome RFI: high mask angle antennas and multiple constellations [6].

(a) Choke ring [15, 16]

(b) Helibowl [16]

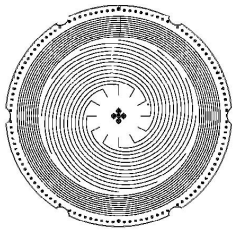

(c) Pinwheel [17]

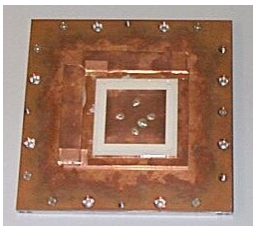

(d) Dual patch [18]

Figure 2. GNSS antennas that can reject signals from low elevation angles.

with the accuracy and integrity requirements defined for a single constellation with a low mask angle antenna.

Figure 2 shows three marketplace antennas (a, b, and c) and a lab-bench antenna (d) that can be manufactured or configured with a high mask angle. As can be seen from the radiation patterns in Figure 3, with a 15° increase in the mask angle, the antenna obtains 10-dB advantage in rejecting signals from the horizon. In general, the higher the mask angle, the greater the attenuation of signals from low elevation angles is.

Although it sounds very reasonable and practical to use HMAAs to overcome RFI, the following two questions remain unclear.

- How much is the optimal mask angle?
- How many satellites (or how many constellations) should be used?

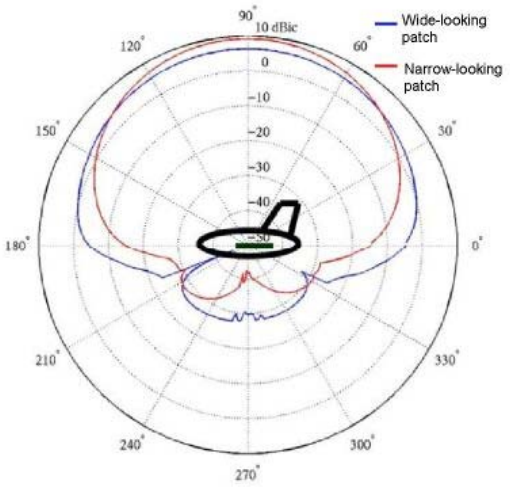

Figure 3. Elevation radiation patterns of a dual-patch antenna [18]. The mask angle of the narrow-looking patch is approximately 15° higher than the wide-looking patch. The narrow-looking patch has a 10-dB advantage in rejecting signals from the horizon.

The objective of this paper is to provide clear guidelines on designing and using HMAAs for overcoming RFI. To this end, the above two questions need be systematically addressed. The fundamental idea of this paper is to employ dilution of precision (DOP) [1] as a performance measure, and find the highest mask angle such that the performance of multiple constellations is not worse than the performance of a single constellation with a standard, low mask angle antenna.

For the rest of this paper, we start with a formal formulation of the problem. Afterward, we theoretically analyze the optimal antenna mask angle. Finally, we conduct simulations to validate the theoretical results.

PROBLEM FORMULATION

The choice of mask angle is a tradeoff between robustness and performance. On one hand, a higher mask angle can better suppress RFI signals coming from low elevation angles. On the other hand, a higher mask angle also rejects useful signals from low elevation GNSS satellites, and thus leads to worse user-satellite geometry, which degenerates accuracy and integrity performance.

The goal of this paper is to find the optimal mask angle such that we can obtain the maximum robustness without sacrificing performance. Mathematically, this goal can be formulated as the following optimization problem:

$$\begin{aligned} &\text{maximize} && \alpha, \\ &\text{subject to} && u(n,\alpha) \geq u(n_0,\alpha_0). \end{aligned} \tag{1}$$

In (1), α is the mask angle for multiple constellations, which include a total of n satellites; α_0 is the mask angle for a single constellation, which includes a total of n_0 satellites; $u(n,\alpha)$ is a utility function quantifying the goodness or performance of satellite geometry. In this paper, the baseline geometry is based on a single GPS constellation of 30 satellites with a 5° mask angle, i.e., $n_0 = 30$ and $\alpha_0 = 5°$.

For most GNSS applications, the utility function $u(n,\alpha)$ is monotonically increasing with respect to n and monotonically decreasing with respect to α. Since multiple constellations contain more satellites than a single constellation, i.e., $n > n_0$, we have $u(n,\alpha_0) > u(n_0,\alpha_0)$. Therefore, there must exist $\alpha^* > \alpha_0$ such that

$$u(n,\alpha^*) = u(n_0,\alpha_0). \tag{2}$$

α^* is the optimal mask angle satisfying (1). This proves that the optimization problem (1) is always feasible, and there must exist a mask angle higher than α_0 for multiple constellations to match the baseline performance.

THEORETICAL ANALYSIS

This section theoretically analyzes the quantitative relationship between the antenna mask angle and the expectation of DOP. To simplify the analysis, we use circles as an approximation of the slightly elliptical satellite orbits, and assume the same range accuracy for all constellations. Since the analysis is based on the concept of global average, we assume that satellites are uniformly distributed on the sphere containing their orbits.

Average number of satellites

Suppose that there are a total of n satellites in a GNSS constellation. As shown in Fig. 4, the average number of satellites is proportional to the area of the spherical cap

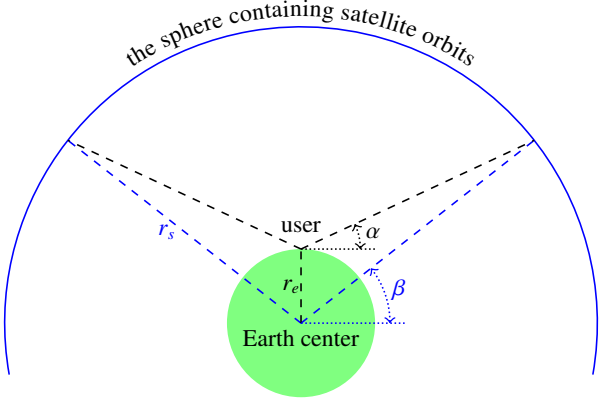

Figure 4. Geometric method for calculating average number of satellites.

above the angle β. By the law of sines, we have

$$\frac{\sin(\alpha + \pi/2)}{r_s} = \frac{\sin(\beta - \alpha)}{r_e}, \tag{3}$$

where α is the antenna mask angle, r_s is the radius of the satellite orbit, and r_e is the Earth radius. Therefore, the angle β is given by

$$\beta = \alpha + \sin^{-1}\Big(\frac{r_e}{r_s}\cos\alpha\Big) = \alpha + \sin^{-1}(\kappa^{-1}\cos\alpha), \tag{4}$$

where $\kappa = r_s/r_e$ is the orbital radius normalized by the Earth radius. For GLONASS, GPS, Compass, and Galileo, $\kappa = 3.998$, 4.175, 4.375, and 4.645, respectively.

The average number of satellites in view is a function of n, α, and κ:

$$\begin{aligned} m(n, \alpha, \kappa) &= \frac{2\pi r_s(r_s - r_s\sin\beta)}{4\pi r_s^2} n \\ &= \frac{n}{2}(1 - \sin[\alpha + \sin^{-1}(\kappa^{-1}\cos\alpha)]). \end{aligned} \tag{5}$$

Fig. 5 shows how the average number of visible satellites varies with the antenna mask angle for three constellation settings. It can be seen that in terms of average number of visible satellites, two constellations can match performance of one with 20-degree higher mask, and three constellations can match performance of one with 32-degree higher mask.

Fig. 5 also shows that although the orbital radius of Galileo is 16% greater than that of GLONASS, the average number of satellites does not show a significant difference. Therefore, in the following analysis, we ignore the difference between orbital radii when discussing multiple constellations.

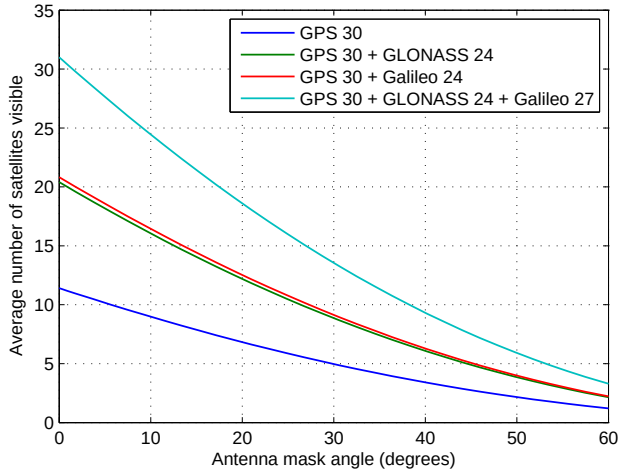

Figure 5. Average number of visible satellites calculated using (5) for three constellation settings: 30 GPS satellites, 30 GPS satellites plus 24 GLONASS satellites, and 30 GPS satellites plus 24 Galileo satellites.

DOP metrics

When the satellites of different constellations can be assumed to have the same range accuracy, DOP simply specifies the multiplicative effect on positioning accuracy due to satellite geometry. When the satellites of different constellations cannot be assumed to have the same range accuracy performance [22–24], weighted DOP (WDOP), also known as KDOP [25, 26], is used in this paper to specify the multiplicative effect on positioning accuracy due to not only satellite geometry but also the range accuracy performance of different constellations.

For interoperable[2] GNSS constellations, the geometry matrix [1] of m visible satellites can be written as

$$G = \begin{pmatrix} \cos\phi_1\cos\theta_1 & \cos\phi_1\sin\theta_1 & \sin\phi_1 & -1 \\ \vdots & \vdots & \vdots & \vdots \\ \cos\phi_m\cos\theta_m & \cos\phi_m\sin\theta_m & \sin\phi_m & -1 \end{pmatrix}, \tag{6}$$

where ϕ_k and θ_k are the elevation and azimuth angles of the kth satellite seen by the user, $k = 1, \ldots, m$. The covariance of positioning errors $\boldsymbol{\varepsilon}$ is given by [1]

$$\mathrm{cov}(\boldsymbol{\varepsilon}, \boldsymbol{\varepsilon}) = (G^{\mathrm{T}}\Sigma^{-1}G)^{-1}, \tag{7}$$

where $\Sigma = \mathrm{cov}(\boldsymbol{\epsilon}, \boldsymbol{\epsilon})$ is the covariance of range errors $\boldsymbol{\epsilon}$. If the range errors of different satellites can be assumed to be independent, the covariance matrix is diagonal,

$$\Sigma = \mathrm{diag}(\sigma_1^2, \ldots, \sigma_k^2). \tag{8}$$

Let σ^2 denote the nominal variance of the range errors of GPS satellites. With the weighting matrix defined as

$$W = \mathrm{diag}(\sigma_1^2/\sigma^2, \ldots, \sigma_k^2/\sigma^2), \tag{9}$$

the covariance of positioning errors can be rewritten as

$$\mathrm{cov}(\boldsymbol{\varepsilon}, \boldsymbol{\varepsilon}) = \sigma^2(G^{\mathrm{T}}W^{-1}G)^{-1}. \tag{10}$$

Then, letting $H = (G^{\mathrm{T}}W^{-1}G)^{-1}$, we have the following weighted DOP metrics:

- Geometric DOP (GDOP) = $\sqrt{H_{11} + H_{22} + H_{33} + H_{44}}$;
- Horizontal DOP (HDOP) = $\sqrt{H_{11} + H_{22}}$;
- Vertical DOP (VDOP) = $\sqrt{H_{33}}$;
- Positional DOP (PDOP) = $\sqrt{H_{11} + H_{22} + H_{33}}$;
- Time DOP (TDOP) = $\sqrt{H_{44}}$.

Since DOP values vary with time and locations, we use global average DOP, namely, the mathematical expectation of DOP, as the utility function $u(n, \alpha)$. Two mask angle and constellation settings have equivalent performance if they yield the same expectation of DOP.

In this paper, our theoretical analysis is based on an idealized model that different constellations have the same range accuracy. In the simulation results, both the idealized model and a more actual model are used.

[2] In this paper, interoperablity means that the reference frames of different GNSS constellations are consistent, and the time offsets between different constellations are known [27].

Lower bound on expectation of DOP

The geometry matrix (6) can be rewritten as

$$G = \begin{pmatrix} \sqrt{1-u_1^2}\cos\theta_1 & \sqrt{1-u_1^2}\sin\theta_1 & u_1 & -1 \\ \vdots & \vdots & \vdots & \vdots \\ \sqrt{1-u_m^2}\cos\theta_m & \sqrt{1-u_m^2}\sin\theta_m & u_m & -1 \end{pmatrix}, \quad (11)$$

where $u_k = \sin\phi_k$ is the sine of the elevation angle of the kth satellite. Since the orbital radius is four times as large as the Earth radius, we consider a further approximation that, on average, the satellites are uniformly distributed on a sphere centered at the user. With such an approximate assumption, both u_k and θ_k are uniformly distributed [28]:

$$u_k \sim \mathcal{U}[\mu, 1], \quad (12)$$

$$\theta_k \sim \mathcal{U}[-\pi, \pi], \quad (13)$$

where $\mu = \sin\alpha$ and α is the antenna mask angle.

Under the assumption that all satellites have the same range accuracy, the expectation of DOP is derived from the diagonal elements of the matrix $\mathrm{E}\,H = \mathrm{E}[(G^{\mathrm{T}}G)^{-1}]$. Unfortunately, it is very difficult to evaluate $\mathrm{E}\,H$ analytically. Instead, we consider $[\mathrm{E}(G^{\mathrm{T}}G)]^{-1}$ here not only because it can be evaluated analytically, but also because it is proven to be a lower bound on $\mathrm{E}[(G^{\mathrm{T}}G)^{-1}]$, as stated by the following theorem.

Theorem 1 (Lower bound on expectation of DOP matrix)**.** *For a random geometry matrix G defined in* (11)*,*

$$\mathrm{E}[(G^{\mathrm{T}}G)^{-1}] \geq [\mathrm{E}(G^{\mathrm{T}}G)]^{-1}, \quad (14)$$

where the operator $X \geq Y$ means that $X - Y$ is positive semidefinite.

A proof of this theorem is shown in Appendix.

Rewriting the geometry matrix in (11) as $G = [g_1, g_2, g_3, g_4]$, where g_i, $i = 1, \ldots, 4$, are random vectors with a length of m, we have

$$\mathrm{E}(G^{\mathrm{T}}G) = [\mathrm{E}\, g_i^{\mathrm{T}} g_j]_{i,j=1,\ldots,4}. \quad (15)$$

For the distributions in (12) and (13), each element of $\mathrm{E}(G^{\mathrm{T}}G)$ is given by

$$\begin{aligned} \mathrm{E}\, g_1^{\mathrm{T}} g_1 = \mathrm{E}\, g_2^{\mathrm{T}} g_2 &= m\,\mathrm{E}(1-u_k^2)\,\mathrm{E}\cos^2\theta_k^2 \\ &= m\frac{2-\mu-\mu^2}{6}, \end{aligned} \quad (16)$$

$$\mathrm{E}\, g_3^{\mathrm{T}} g_3 = m\,\mathrm{E}(u_k^2) = m\frac{1+\mu+\mu^2}{3}, \quad (17)$$

$$\mathrm{E}\, g_4^{\mathrm{T}} g_4 = m, \quad (18)$$

$$\mathrm{E}\, g_3^{\mathrm{T}} g_4 = \mathrm{E}\, g_4^{\mathrm{T}} g_3 = -m\,\mathrm{E}\, u_k = -m\frac{1+\mu}{2}, \quad (19)$$

$$\begin{aligned} \mathrm{E}\, g_1^{\mathrm{T}} g_2 = \mathrm{E}\, g_2^{\mathrm{T}} g_1 &= \mathrm{E}\, g_1^{\mathrm{T}} g_3 = \mathrm{E}\, g_3^{\mathrm{T}} g_1 \\ &= \mathrm{E}\, g_1^{\mathrm{T}} g_4 = \mathrm{E}\, g_4^{\mathrm{T}} g_1 \\ &= \mathrm{E}\, g_2^{\mathrm{T}} g_3 = \mathrm{E}\, g_3^{\mathrm{T}} g_2 \\ &= \mathrm{E}\, g_2^{\mathrm{T}} g_4 = \mathrm{E}\, g_4^{\mathrm{T}} g_2 = 0, \end{aligned} \quad (20)$$

where the average number of satellites m can be calculated from (5). The lower bound matrix is hence given by

$$\begin{aligned} [\mathrm{E}(G^{\mathrm{T}}G)]^{-1} &= \frac{1}{m}\begin{pmatrix} \frac{2-\mu-\mu^2}{6} & 0 & 0 & 0 \\ 0 & \frac{2-\mu-\mu^2}{6} & 0 & 0 \\ 0 & 0 & \frac{1+\mu+\mu^2}{3} & -\frac{1+\mu}{2} \\ 0 & 0 & -\frac{1+\mu}{2} & 1 \end{pmatrix}^{-1} \\ &= \frac{2}{m(1-\mu)}\begin{pmatrix} \frac{3}{2+\mu} & 0 & 0 & 0 \\ 0 & \frac{3}{2+\mu} & 0 & 0 \\ 0 & 0 & \frac{6}{1-\mu} & 3 \\ 0 & 0 & 3 & \frac{2(1+\mu+\mu^2)}{1-\mu} \end{pmatrix}. \end{aligned} \quad (21)$$

Now we can obtain the lower bound on the expectation of the five DOP metrics:

$$\mathrm{E}(\mathrm{GDOP}^2) \geq \frac{4}{m}\cdot\frac{9+(1+\mu+\mu^2)(2+\mu)}{(2+\mu)(1-\mu)^2}, \quad (22)$$

$$\mathrm{E}(\mathrm{HDOP}^2) \geq \frac{4}{m}\cdot\frac{3}{(2+\mu)(1-\mu)}, \quad (23)$$

$$\mathrm{E}(\mathrm{VDOP}^2) \geq \frac{4}{m}\cdot\frac{3}{(1-\mu)^2}, \quad (24)$$

$$\mathrm{E}(\mathrm{PDOP}^2) \geq \frac{4}{m}\cdot\frac{9}{(2+\mu)(1-\mu)^2}, \quad (25)$$

$$\mathrm{E}(\mathrm{TDOP}^2) \geq \frac{4}{m}\cdot\frac{1+\mu+\mu^2}{(1-\mu)^2}. \quad (26)$$

Optimal mask angles

Fig. 6 shows the lower bound on expectation of GDOP calculated using (22) for one constellation comprised of 30 satellites, two constellations comprised of 54 satellites, and three constellations comprised of 84 satellites. It can be seen that two constellations can match the GDOP performance

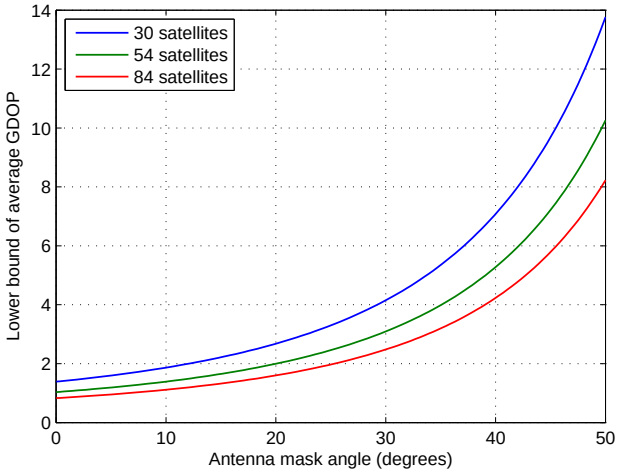

Figure 6. Lower bound on expectation of GDOP calculated using (22) for one constellation comprised of 30 satellites, two constellations comprised of 54 satellites, and three constellations comprised of 84 satellites.

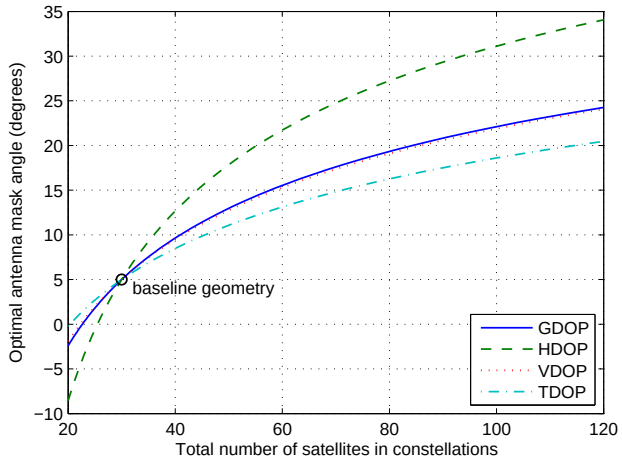

Figure 7. Relationship between the optimal antenna mask angle and the total number of satellites for achieving GDOP, HDOP, VDOP, and TDOP of the baseline geometry.

of one with a mask angle of approximately 15°, and three constellations can match the GDOP performance of one with a mask angle of approximately 21°.

Fig. 7 shows relationship between the optimal antenna mask angle and the total number of satellites for achieving GDOP, HDOP, VDOP, and TDOP of the baseline geometry. It can be seen that given a 15° mask angle, 44 satellites are required to achieve the baseline HDOP performance, 57 satellites are required to achieve the baseline GDOP and VDOP performance, and 71 satellites are required to achieve the baseline TDOP performance. This shows that using high mask angle antennas with multiple constellations is more beneficial to users interested in positioning accuracy (especially horizontal accuracy) than users interested in time transfer accuracy.

Fig. 7 also shows that the optimal mask angles to achieve the baseline VDOP and GDOP performance are very close. The first reason is that VDOP values are usually larger than HDOP and TDOP values, and thus dominate GDOP values. The second reason is that for an increasing mask angle, the HDOP value increases slower than the VDOP value, while the TDOP value increases faster than the VDOP value. The difference between the increasing slopes of HDOP and TDOP approximately compensate each other, leaving the GDOP values almost only affected by the VDOP values.

Moreover, the concavity of all the curves in Fig. 7 implies diminishing marginal utility: the gain of mask angle due to adding one more satellite decreases as the total number of satellites increases. Therefore, introducing a third constellation is not as beneficial as introducing a second constellation.

SIMULATION RESULTS

Simulation Setting

All the results presented in this section are based on the simulation setting listed below.

- Orbit parameters:

  GPS broadcast almanacs of 30 usable GPS satellites on 23 January 2013.

  GLONASS broadcast almanacs of 24 active GLONASS-M satellites on 23 January 2013.

  Galileo planned orbits of 27 Galileo satellites [29].
- Baseline geometry: the GPS constellation of 30 satellites with a 5° mask angle.
- Temporal sampling: 1 sample per 29 minutes over 2 days.
- Spatial sampling: 1807 points nearly evenly distributed on the Earth, as shown in Fig. 8.
- Range accuracy:

  Model 1 the same range accuracy for all constellations.

  Model 2 6 meters for GPS and Galileo; 8 meters for GLONASS (detailed below).

In order to see how range accuracy affect optimal mask angle, this paper considers the following constellation-specific range error model:

- Signal-in-space (SIS) errors: 3 meters for GPS [1] and Galileo; 6 meters for GLONASS.
- Atmospheric propagation modeling errors: 6 meters [1].
- Receiver noise and multipath: 1 meter for GPS [1] and Galileo; 2 meters for GLONASS.
- Total pseudorange measurement errors: 6 meters for GPS and Galileo; 8 meters for GLONASS.

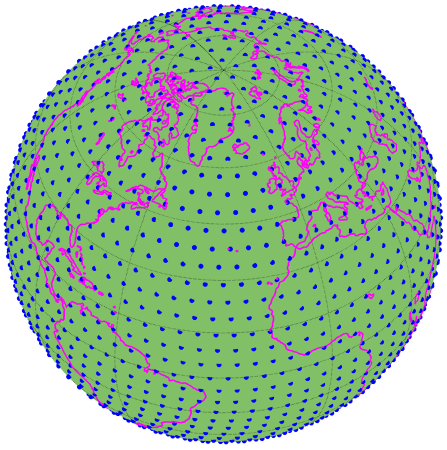

Figure 8. DOP values are computed for 1807 points nearly evenly distributed on the Earth. The spherical distance between any two neighbor points is roughly 5°.

In the above list, Galileo is arbitrarily assumed to be on a par with GPS. GLONASS is assumed to have a worse range accuracy because the GLONASS SIS errors are roughly twice as large as those of GPS [23, 24], and the chip rate of GLONASS civil signals is half of the chip rate of GPS and Galileo civil signals.

In fact, Galileo has not yet been fully operational and their SIS accuracy performance is unknown. Today's GPS SIS accuracy is actually much better than 3 meters [22]. The ionospheric errors for a single-frequency receiver can be highly variable depending on the user location and satellite elevation angle. In addition, the noise and multipath can also vary with the satellite elevation angle [30]. Nevertheless, in this paper, the main purpose of considering weighted DOP in simulations is to check whether range accuracy can significantly affect the optimal mask angle. Since a sophisticated, accurate range error model is unnecessary for this purpose (and even impossible because the Galileo SIS accuracy performance is unknown), we use this very simple error model despite its crudeness and inaccuracy.

Optimal Mask Angles for Different DOP Metrics and Different Range Error Models

Table 1 shows the optimal mask angles for five different DOP metrics, two different constellation settings, and two different range accuracy models. It can be seen that 54 satellites (30 GPS satellites and 24 GLONASS satellites) can matches the baseline GDOP performance with 10° higher mask if GLONASS range accuracy can be assumed to be as good as GPS. If the second range accuracy model is used, 54 satellites can match the GDOP performance of GPS-only with 7° higher mask. When there are 81 satellites (30 GPS satellites, 24 GLONASS satellites, and 27 Galileo satellites), the optimal antenna mask angle to match the baseline GDOP performance is approximately 21.1 and 19.4 degrees for the first and second range accuracy models, respectively. Needless to say, range accuracy plays an important role in determining the optimal mask angle.

Moreover, Table 1 shows that with increased number of satellites, a high mask angle can match the HDOP performance more easily than the TDOP performance. Table 1 also shows that the optimal mask angles to achieve the baseline VDOP and GDOP performance are very close. These observations highly agree with our theoretical analysis.

Comparison between theoretical and numerical results

Figure 9 compares theoretical and numerical results. The markers show the optimal mask angles from the simulation results for the first range accuracy model. The theoretical equal-performance curves are the same as Figure 7. It can be seen that the theoretical results highly match numerical results, with less than 2-degree difference in optimal mask angles. This validates our theoretical results, and demonstrates that our lower bound on expectation of DOP is tight.

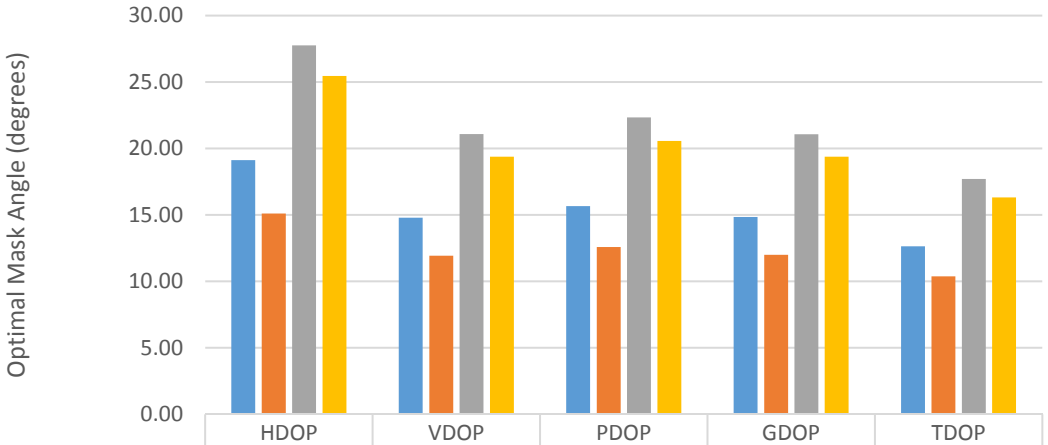

	HDOP	VDOP	PDOP	GDOP	TDOP
54 sats, Model 1	19.12	14.79	15.67	14.84	12.64
54 sats, Model 2	15.10	11.92	12.58	11.99	10.38
81 sats, Model 1	27.75	21.08	22.34	21.06	17.71
81 sats, Model 2	25.46	19.37	20.56	19.37	16.31

Table 1. Optimal mask angles for five different DOP metrics, two different constellation settings, and two different range accuracy models.

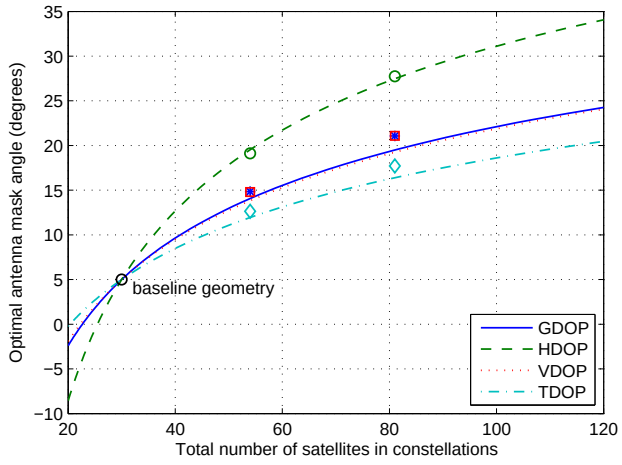

Figure 9. Comparison between theoretical and numerical results. The markers show the optimal mask angles from the simulation results for the first range accuracy model. The theoretical equal-performance curves are the same as Figure 7.

CONCLUDING REMARKS

In this paper, we have thoroughly treated a new method to overcome RFI from terrestrial sources—using HMAAs and multiple GNSS constellations. We have defined the optimal mask angle to be the highest mask angle such that the positioning performance of multiple constellations can match the performance of a single constellation with low mask angle antennas. We have discovered and proved a lower bound on expectation of DOP. With this lower bound, we derived closed-form formulas to calculate optimal mask angles for different DOP metrics. Our numerical results have validated the theoretical analysis.

Both theoretical and numerical results show that GPS + GLONASS can match performance of GPS with 5–14° higher mask, and GPS + GLONASS + Galileo can match performance of GPS with 11–23° higher mask, where the exact value depends on the constellation setting, DOP metric, and range accuracy model. Moreover, the results show diminishing marginal utility, i.e., the gain of mask angle due to adding one more satellite decreases as the total number of satellites increases. Additional, this method is more beneficial to users interested in positioning accuracy (especially horizontal accuracy) than users interested in time transfer accuracy.

Overall, using HMAAs is an effective method for multi-constellation GNSS users to overcome RFI. The results presented in this paper provide guidelines on designing HMAAs and using this method in practice. The following topics are not covered in this paper, but may be worth being explored further in a future paper.

- A more sophisticated range error model considering the satellite elevation angles and user's locations;
- Actual data from multi-constellation GNSS receivers to validate the optimal mask angles found in this paper.

APPENDIX: PROOF OF THEOREM 1

There are a few approaches to proving Theorem 1. One of the simplest proofs is based on recent results on the Cauchy–Schwarz inequality for the expectation of random matrices [31, 32]:

Lemma 1 (Cauchy–Schwarz inequality [31, 32])**.** *Let* $A \in \mathbb{R}^{n\times p}$ *and* $B \in \mathbb{R}^{n\times p}$ *be random matrices such that* $\mathrm{E}\,\|A\|^2 < \infty$, $\mathrm{E}\,\|B\|^2 < \infty$, *and* $\mathrm{E}(A^{\mathrm{T}}A)$ *is non-singular. Then*

$$\mathrm{E}(B^{\mathrm{T}}B) \geq \mathrm{E}(B^{\mathrm{T}}A)[\mathrm{E}(A^{\mathrm{T}}A)]^{-1}\,\mathrm{E}(A^{\mathrm{T}}B). \tag{27}$$

With the substitutions $A = G$ and $B = G(G^{\mathrm{T}}G)^{-1}$ into the above inequality, we have

$$U = \mathrm{E}[(G^{\mathrm{T}}G)^{-1}] \geq V = [\mathrm{E}(G^{\mathrm{T}}G)]^{-1}, \tag{28}$$

which already proves Theorem 1.

Since the diagonal elements of a positive semidefinite matrix must be non-negative, we have

$$U_{ii} \geq V_{ii}, \quad \forall i = 1, \ldots, dN_S, \tag{29}$$

where $U = [U_{ij}]$ and $V = [V_{ij}]$. In particular, the expectation of GDOP, $\sqrt{\mathrm{trace}(U)}$, has a lower bound $\sqrt{\mathrm{trace}(V)}$.

REFERENCES

[1] P. Misra and P. Enge, *Global Positioning System: Signals, Measurements, and Performance*, 2nd ed. Lincoln, MA: Ganga-Jamuna Press, 2006.

[2] Fox News, "South Korea claims North Korea GPS jamming is affecting civilian flights," May 2012. [Online]. Available: http://www.foxnews.com/world/2012/05/02/south-korea-claims-north-korea-gps-jamming-is-affecting-civilian-flights

[3] J. R. Clynch, A. A. Parker, R. W. Adler, W. R. Vincent, P. McGill, and G. Badger, "The hunt for RFI," *GPS World*, vol. 14, no. 1, pp. 16–22, Jan. 2003.

[4] P. W. Ward, "GNSS robustness: The interference challenge," in *Proceedings of the 23rd International Technical Meeting of the Satellite Division of the Institute of Navigation (ION GNSS 2010)*, Portland, OR, Sep. 2010, pp. 69–97.

[5] T. Kraus, R. Bauernfeind, and B. Eissfeller, "Survey of in-car jammers—analysis and modeling of the RF signals and IF samples (suitable for active signal cancelation)," in *Proceedings of the 24th International*

Technical Meeting of the Satellite Division of the Institute of Navigation (ION GNSS 2011), Portland, OR, Sep. 2011, pp. 430–435.

[6] S. Pullen, G. X. Gao, C. Tedeschi, and J. Warburton, "The impact of uninformed RF interference on GBAS and potential mitigations," in *Proceedings of the 2012 International Technical Meeting of the Institute of Navigation (ION ITM 2012)*, Newport Beach, CA, Jan. 2012, pp. 780–789.

[7] G. X. Gao, L. Heng, A. Hornbostel, H. Denks, M. Meurer, T. Walter, and P. Enge, "DME/TACAN interference mitigation for GNSS: Algorithms and flight test results," *GPS Solutions*, Nov. 2012.

[8] N. D. Pham, "The economic benefits of commercial GPS use in the U.S. and the costs of potential disruption," NDP Consulting, Tech. Rep., Jun. 2011. [Online]. Available: http://www.saveourgps.org/pdf/GPS-Report-June-22-2011.pdf

[9] M. V. Tazebay and A. N. Akansu, "Adaptive subband transforms in time-frequency excisers for DSSS communications systems," *IEEE Transactions on Signal Processing*, vol. 43, no. 11, pp. 2776–2782, Nov. 1995.

[10] A. S. Ayaz, R. Bauernfeind, T. Pany, and B. Eissfeller, "Time-frequency based intentional interference suppression techniques in GNSS receivers," in *Proceedings of the 25th International Technical Meeting of the Satellite Division of the Institute of Navigation (ION GNSS 2012)*, Nashville, TN, Sep. 2012.

[11] D.-J. Moelker and Y. Bar-Ness, "An optimal array processor for GPS interference cancellation," in *15th AIAA/IEEE Digital Avionics Systems Conference*, Oct. 1996, pp. 285–291.

[12] D. De Lorenzo, J. Gautier, J. Rife, P. Enge, and D. Akos, "Adaptive array processing for GPS interference rejection," in *Proceedings of the 18th International Technical Meeting of the Satellite Division of the Institute of Navigation (ION GNSS 2005)*, Long Beach, CA, Sep. 2005, pp. 618–627.

[13] Y.-H. Chen, J.-C. Juang, J. Seo, S. Lo, D. M. Akos, D. De Lorenzo, and P. Enge, "Design and implementation of real-time software radio for anti-interference GPS/WAAS sensors," *Sensors*, vol. 12, no. 10, pp. 13 417–13 440, 2012.

[14] D. De Lorenzo, "Navigation accuracy and interference rejection for GPS adaptive antenna arrays," Ph.D. dissertation, Stanford University, 2007.

[15] J. M. Tranquilla, J. P. Carr, and H. M. Al-Rizzo, "Analysis of a choke ring groundplane for multipath control in Global Positioning System (GPS) applications," *IEEE Transactions on Antennas and Propagation*, vol. 42, no. 7, pp. 905–911, Jul. 1994.

[16] G. Wong, Y.-H. Chen, R. E. Phelts, T. Walter, and P. Enge, "Measuring code-phase differences due to inter-satellite hardware differences," in *Proceedings of the 25th International Technical Meeting of the Satellite Division of the Institute of Navigation (ION GNSS 2012)*, Nashville, TN, Sep. 2012, pp. 2150–2158.

[17] W. Kunysz, "High performance GPS pinwheel antenna," in *Proceedings of the 13th International Technical Meeting of the Satellite Division of the Institute of Navigation (ION GPS 2000)*, Salt Lake City, UT, Sep. 2000, pp. 2506–2511.

[18] F. Bauregger, T. Walter, D. Akos, and P. Enge, "A novel dual-patch anti-jam GPS antenna," in *Proceedings of the 58th Annual Meeting of the Institute of Navigation*, Albuquerque, NM, Jun. 2002, pp. 516–522.

[19] P. Enge and A. J. Van Dierendonck, "Wide area augmentation system," in *Global Positioning System: Theory and Applications*, B. Parkinson, J. Spilker, P. Axelrad, and P. Enge, Eds. Washington, DC: American Institute of Aeronautics and Astronautics, 1996, vol. II, pp. 117–142.

[20] T. Walter, P. Enge, and A. Hansen, "A proposed integrity equation for WAAS MOPS," in *Proceedings of the 10th International Technical Meeting of the Satellite Division of the Institute of Navigation (ION GPS 1997)*, Kansas City, MO, Sep. 1997, pp. 475–484.

[21] RTCA Special Committee 159, *Minimum Operational Performance Standards for Global Positioning System/Wide Area Augmentation System Airborne Equipment*. RTCA DO-229D, Dec. 2006.

[22] L. Heng, G. X. Gao, T. Walter, and P. Enge, "Statistical characterization of GPS signal-in-space errors," in *Proceedings of the 2011 International Technical Meeting of the Institute of Navigation (ION ITM 2011)*, San Diego, CA, Jan. 2011, pp. 312–319.

[23] ——, "Statistical characterization of GLONASS broadcast ephemeris errors," in *Proceedings of the 24th International Technical Meeting of the Satellite Division of the Institute of Navigation (ION GNSS 2011)*, Portland, OR, Sep. 2011, pp. 3109–3117.

[24] ——, "Statistical characterization of GLONASS broadcast clock errors and signal-in-space errors," in *Proceedings of the 2012 International Technical Meet-*

ing of the Institute of Navigation (ION ITM 2012), Newport Beach, CA, Jan. 2012, pp. 1697–1707.

[25] U.S. Coast Guard Navigation Center, *Navstar GPS User Equipment Introduction*, Sep. 1996. [Online]. Available: http://www.navcen.uscg.gov/pubs/gps/gpsuser/gpsuser.pdf

[26] H. Sairo, D. Akopian, and J. Takala, "Weighted dilution of precision as quality measure in satellite positioning," *IEE Proceedings Radar, Sonar and Navigation*, vol. 150, no. 6, pp. 430–436, Dec. 2003.

[27] G. Hein, "Gnss interoperability: Achieving a global system of systems or 'does everything have to be the same?'," *Inside GNSS*, vol. 1, no. 1, Jan. 2006.

[28] E. W. Weisstein, "Sphere point picking," *MathWorld—A Wolfram Web Resource*. [Online]. Available: http://mathworld.wolfram.com/SpherePointPicking.html

[29] European Union, *European GNSS (Galileo) Open Service Signal In Space Interface Control Document*, Sep. 2010.

[30] A. Jahn, H. Bischl, and G. Heiss, "Channel characterisation for spread spectrum satellite communications," in *IEEE 4th International Symposium on Spread Spectrum Techniques and Applications*, vol. 3, Sep. 1996, pp. 1221–1226.

[31] G. Tripathi, "A matrix extension of the Cauchy-Schwarz inequality," *Economics Letters*, vol. 63, no. 1, pp. 1–3, 1999.

[32] P. Lavergne, "A Cauchy-Schwarz inequality for expectation of matrices," Simon Fraser University, Tech. Rep., Nov. 2008.